

RPA-CPA theory for magnetism in disordered Heisenberg binary systems with long-range exchange integrals

G. Bouzerar and P. Bruno

Max-Planck-Institute für Mikrostrukturphysik, Weinberg 2, D-06120 Halle, Germany

(Received 7 February 2002; published 28 June 2002)

We present a theory based on Green's-function formalism to study magnetism in disordered Heisenberg systems with long-range exchange integrals. Disordered Green's functions are decoupled within the Tyablicov scheme and solved with a coherent potential approximation (CPA) method. The CPA method is the extension of Blackman-Esterling-Beck approach to systems with an environmental disorder term which uses cumulant summation of the single-site noncrossing diagrams. The crucial point is that we are able to treat simultaneously and self-consistently the random-phase approximation (RPA) and CPA loops. It is shown that the summation of the s -scattering contribution can always be performed analytically, while the p, d, f, \dots contributions are difficult to handle in the case of long-range coupling. To overcome this difficulty we propose and provide a test of a simplified treatment of these terms. In the case of the three-dimensional disordered nearest-neighbor Heisenberg system, a good agreement between the simplified treatment and the full calculation is achieved. Our theory allows us in particular to calculate the Curie temperature, the spectral functions, and the temperature dependence of the magnetization of each constituent as a function of concentration of impurity. Additionally it is shown that a virtual crystal treatment fails even at low impurity concentration.

DOI: 10.1103/PhysRevB.66.014410

PACS number(s): 75.10.-b, 75.25.+z, 75.50.Cc, 71.10.-w

I. INTRODUCTION

The coherent potential approximation (CPA) is widely used to study the effect of disorder in crystals (for reviews see Refs. 1 and 2). The CPA was initially developed independently by Soven³ and Taylor⁴ to study systems with only *diagonal* disorder. Using a 2×2 formulation, a generalization to the presence of *off-diagonal* disorder was provided by Blackman, Esterling, and Berk (BEB).^{5,6} In these approaches the main idea is to replace the system by an effective medium which is determined by the condition that the averaged T matrix of a single impurity immersed in the effective medium is zero. An alternative approach is based on cumulant expansion.^{7,8} This latter method has the advantage that it can handle the *environmental* disorder term which is characteristic of the Goldstone's systems (phonons, magnons). The proper treatment of the environmental disorder term, by using the cumulant expansion method, was used by Lage and Stinchcombe,⁹ who studied the diluted Ising problem ($S = 1/2$). Later, using the 2×2 matrix method of Blackman, Esterling, and Berk, the method was extended by Whitelaw¹⁰ to the phonon problem. In their calculations the coupling and locator are fixed quantities and restricted to nearest-neighbor exchange couplings. It is well known that magnetism in clean ferromagnetic systems can be tackled with Green's-function formalism using Tyablicov decoupling procedure [random-phase approximation (RPA)]. This method goes beyond a simple mean field since it includes quantum fluctuations. Additionally, it fulfills the Goldstone and Mermin-Wagner theorems which is not the case of a mean-field treatment. In the case of clean systems, combining first-principle calculations to evaluate the exchange integrals and RPA method, it was shown that one can provide a satisfactory Curie temperature for Co and Fe,¹¹ while, a simple mean-field calculation largely overestimates the Curie tem-

perature. It is our objective to provide in this paper a generalization of the RPA method to the disordered systems. We show that by combining in a self-consistent manner the RPA method and the CPA treatment of the disorder we are able to calculate Curie temperature, magnetization of the different constituents, spectral weights, etc. The CPA treatment is done in a similar way as done by Lage and Stinchcombe and by Whitelaw. However, due to the Tyablicov decoupling scheme for the disordered Green's functions, the locators and the effective exchange integrals are temperature dependent and have to be determined self-consistently for a given temperature.

The paper is organized as follows. In the first section we derive after the Tyablicov decoupling scheme the disordered binary alloy Green's function which includes *diagonal*, *off-diagonal*, and *environmental* disorder. In Sec. II, we perform the calculation of the averaged Green's functions for the A (respectively B) atom. In Sec. III, by generalizing Callen's formula we derive the equations for the magnetizations m_A , m_B , and for the Curie temperature. In Sec. IV, we propose an alternative simplified treatment of the p, d, \dots scattering contribution to the self-energy to the case of system with long-range exchange coupling. Finally in Sec. V we present some numerical results and proceed to a test of our approximation of the self-energy contribution of the higher scattering terms.

II. DISORDERED GREEN'S FUNCTION AND RPA DECOUPLING SCHEME

We study the magnetism in a binary alloy $A_{1-c}B_c$; A and B can be either magnetic ions or nonmagnetic. We denote their spin, respectively, S_A and S_B . The total Hamiltonian reads

$$\hat{H} = \sum_{ij} -J_{ij} \mathbf{S}_i \cdot \mathbf{S}_j - \sum_i D_i (S_i^z)^2 - B \sum_i g \mu_i (S_i^z), \quad (1)$$

where the J_{ij} and D_i are random variables: $J_{ij} = J_{ij}^{\lambda\lambda'} = J_{|i-j|}^{\lambda\lambda'}$ with the probability $P_i^\lambda P_j^{\lambda'}$ where $P_i^\lambda = c_\lambda$ is the probability that the site i is occupied by a λ atom (c_λ concentration of a λ atom).¹² Similarly $D_i = D_\lambda$ with probability P_i^λ . The exchange integrals are assumed to be long range, and our study is not restricted to the nearest-neighbor Heisenberg model. The second term which describes anisotropy is only relevant in the case of two-dimensional (2D) systems to get a nonzero Curie temperature T_c (Mermin-Wagner theorem). However, in the case of 3D systems the contribution of this term can be neglected. We also include the effect of an external magnetic field.

Let us consider the following retarded Green's function:

$$G_{ij}^{+-}(t) = -i\theta(t) \langle [S_i^+(t), S_j^-(0)] \rangle, \quad (2)$$

where $\langle \dots \rangle$ denotes the statistical average at temperature T ,

$$\langle \hat{O} \rangle = \frac{1}{Z} \text{Tr}(e^{-\beta \hat{H}} \hat{O}), \quad (3)$$

where $Z = \text{Tr}(e^{-\beta \hat{H}})$.

$G_{ij}^{+-}(t)$'s Fourier transform in Energy space is

$$\langle\langle S_i^+; S_j^- \rangle\rangle = G_{ij}^{+-}(\omega) = \int_{-\infty}^{+\infty} G_{ij}^{+-}(t) e^{i\omega t} dt. \quad (4)$$

Its equation of motion reads

$$\omega G_{ij}^{+-}(\omega) = 2m_i \delta_{ij} + \langle\langle [S_i^+, H]; S_j^- \rangle\rangle, \quad (5)$$

where $m_i = \langle S_i^z \rangle$, or $m_i = m_A$ (respectively m_B) if $i = A$ (respectively $i = B$).

After expanding the second term on the right side of the equality we obtain

$$(\omega - g \mu_i B) G_{ij}^{+-}(\omega) = 2m_i \delta_{ij} - \sum_l J_{il} \langle\langle S_i^z S_l^+ - S_i^+ S_l^z; S_j^- \rangle\rangle + D_i \langle\langle S_i^z S_i^+ + S_i^+ S_i^z \rangle\rangle. \quad (6)$$

The next step consists of decoupling the higher-order Green's function. For the second term we use the standard Tyablicov decoupling¹³ (equivalent to RPA). The last term due to anisotropy is somehow more complicated since on-site correlations are involved. Following the approach discussed in Ref. 14 we adopt for this term the Anderson-Callen decoupling scheme:¹⁵

$$D_i \langle\langle S_i^+ S_i^z + S_i^z S_i^+ \rangle\rangle = 2D_i \gamma_i m_i, \quad (7)$$

where

$$\gamma_i = 1 - \frac{1}{2S^2} [S_i(S_i + 1) - \langle (S_i^z)^2 \rangle]. \quad (8)$$

After simplification we find

$$G_{ij}^{+-} = g_i \delta_{ij} + g_i \sum_l \Phi_{il} G_{lj}^{+-} - \epsilon g_i \left(\sum_l \Psi_{il} \right) G_{ij}^{+-}, \quad (9)$$

where $\phi_{il} = -1/2J_{il}$ and $\Psi_{il} = -1/2J_{il}(m_l/m_i)$ and g_i denotes the locator: $g_i = g_A^0$ (respectively g_B^0) if $i = A$ (respectively $i = B$),

$$g_\lambda^0(E) = \frac{\frac{m_\lambda}{m}}{E - g \mu_\lambda B / 2m - D_\lambda \gamma_\lambda \frac{m_\lambda}{m}}, \quad (10)$$

where $\lambda = A$ or B . For convenience, we have also introduced the reduced variable $E = \omega/2m$; m denotes the averaged magnetization: $m = \sum_\lambda c_\lambda m_\lambda$. The term which is proportional to ϵ comes from the environmental disorder term. This term is crucial to recover the Goldstone mode and requires to be treated very carefully. We have introduced the coefficient ϵ which is in principle equal to 1, in order to follow the influence of the environmental disorder term during the calculations. Note also that this term appears because of RPA decoupling. If $\epsilon = 0$ Eq. 9 is analogous to the propagator of an electron in a disordered medium with *on-site* potential and random long-range hopping terms $t_{il} = \Phi_{il}$ (*off-diagonal* disorder). In this case the problem can be solved just within the BEB formalism. However, one should stress that the BEB formalism does not apply when the environmental term is present. Note also that in our model the locator g_λ^0 , Ψ_{il} , and γ_i are all temperature dependent, thus CPA and RPA loops have to be treated simultaneously in a self-consistent manner.

III. CUMULANT EXPANSION METHOD FOR THE AVERAGED GREEN'S FUNCTIONS

As it was done in Ref. 10, the basic idea is to write Eq. (9) as a locator expansion in BEB manner.⁵ We define the random variable p_i : $p_i = 1$ if A is at site i or $p_i = 0$ if i is occupied by a B ion. Therefore the locator reads

$$g_i = p_i g_A^0 + (1 - p_i) g_B^0 = g_i^A + g_i^B \quad (11)$$

and

$$\phi_{il} = p_i J_{il}^{AA} p_l + p_i J_{il}^{AB} (1 - p_l) + (1 - p_i) J_{il}^{AB} p_l + (1 - p_i) J_{il}^{BB} (1 - p_l). \quad (12)$$

Similarly,

$$\Psi_{il} = p_i J_{il}^{AA} p_l + p_i J_{il}^{AB,1} (1 - p_l) + (1 - p_i) J_{il}^{AB,2} p_l + (1 - p_i) J_{il}^{BB} (1 - p_l), \quad (13)$$

where $J_{il}^{AB,1} = (m_B/m_A) J_{il}^{AB}$ and $J_{il}^{AB,2} = (m_A/m_B) J_{il}^{AB}$.

The Green's functions are expressed in terms of a 2×2 matrix and one gets for the equation of motion

$$\mathbf{G}_{ij} = \begin{pmatrix} g_i^A & 0 \\ 0 & g_i^B \end{pmatrix} \delta_{ij} + \begin{pmatrix} g_i^A & 0 \\ 0 & g_i^B \end{pmatrix} \sum_m \begin{pmatrix} J_{im}^{AA} & J_{im}^{AB} \\ J_{im}^{AB} & J_{im}^{BB} \end{pmatrix} \begin{pmatrix} G_{mj}^{AA} & G_{mj}^{AB} \\ G_{mj}^{BA} & G_{mj}^{BB} \end{pmatrix} \\ - \epsilon \begin{pmatrix} g_A^0 & 0 \\ 0 & g_B^0 \end{pmatrix} \begin{pmatrix} J^{AB,1} + \sum_l (J_{il}^{AA} - J_{il}^{AB,1}) p_l & 0 \\ 0 & J^{BB} + \sum_l (J_{il}^{AB,2} - J_{il}^{BB}) p_l \end{pmatrix} \begin{pmatrix} G_{ij}^{AA} & G_{ij}^{AB} \\ G_{ij}^{BA} & G_{ij}^{BB} \end{pmatrix}. \quad (14)$$

We have defined the variables $J^{AB,1} = \sum_l J_{il}^{AB,1}$ and $J^{BB} = \sum_l J_{il}^{BB}$.

The aim is to expand this expression into a product of the p factors, which can then be averaged over disorder by expanding into cumulants. For that purpose we separate out the factors and introduce a new variable ρ_i by $p_i = \rho_i + c$ (where $c_A = c$). The idea is to separate out the virtual crystal part,

$$\mathbf{g}_i = \rho_i \begin{pmatrix} g_A^0 & 0 \\ 0 & -g_B^0 \end{pmatrix} + \begin{pmatrix} c g_A^0 & 0 \\ 0 & (1-c) g_B^0 \end{pmatrix}. \quad (15)$$

There is still the environmental term which is more difficult to handle. As it was done by Lage and Stinchcombe⁹, by converting into \mathbf{k} space the calculations become easier to perform.

We define the Fourier transform by

$$\mathbf{G}'_{\mathbf{k}\mathbf{k}'} = \sum_{ij} \exp(i\mathbf{k} \cdot \mathbf{r}_i) \exp(-i\mathbf{k}' \cdot \mathbf{r}_j) \mathbf{G}_{ij}. \quad (16)$$

After some manipulation one gets

$$\mathbf{G}_{\mathbf{k}\mathbf{k}'} = \mathbf{G}_{\mathbf{k}}^{vc} \rho_{\mathbf{k}-\mathbf{k}'} + \mathbf{G}_{\mathbf{k}}^{vc} \begin{pmatrix} c & 0 \\ 0 & c-1 \end{pmatrix} \\ \times \delta_{\mathbf{k}-\mathbf{k}'} + \mathbf{G}_{\mathbf{k}}^{vc} \frac{1}{N} \sum_{\mathbf{q}} \rho_{\mathbf{k}-\mathbf{q}} \mathbf{V}_{\mathbf{k}\mathbf{q}} \mathbf{G}_{\mathbf{q}\mathbf{k}'}, \quad (17)$$

where the 2×2 matrix $\mathbf{V}_{\mathbf{k}\mathbf{q}}$ is defined by

$$\mathbf{V}_{\mathbf{k}\mathbf{q}} = \begin{pmatrix} J_{\mathbf{q}}^{AA} - \epsilon(J_{\mathbf{k}-\mathbf{q}}^{AA} - J_{\mathbf{k}-\mathbf{q}}^{AB,1}) & J_{\mathbf{q}}^{AB} \\ J_{\mathbf{q}}^{AB} & J_{\mathbf{q}}^{BB} - \epsilon(J_{\mathbf{k}-\mathbf{q}}^{BB} - J_{\mathbf{k}-\mathbf{q}}^{AB,2}) \end{pmatrix} \quad (18)$$

and the virtual-crystal Green's function $\mathbf{G}_{\mathbf{k}}^{vc}$,

$$[\mathbf{G}_{\mathbf{k}}^{vc}]^{-1} = \mathbf{M}_0 - c \mathbf{M}_1, \quad (19)$$

where the matrices \mathbf{M}_0 and \mathbf{M}_1 are

$$\mathbf{M}_0 = \begin{pmatrix} (g_A^0)^{-1} & 0 \\ 0 & -(g_B^0)^{-1} \end{pmatrix} + \begin{pmatrix} \epsilon J_{\mathbf{k}}^{AB,1} & 0 \\ J_{\mathbf{k}}^{AB} & J_{\mathbf{k}}^{BB} - \epsilon J_{\mathbf{k}}^{BB} \end{pmatrix} \quad (20)$$

and

$$\mathbf{M}_1 = \begin{pmatrix} J_{\mathbf{k}}^{AA} - \epsilon(J_{\mathbf{k}}^{AA} - J_{\mathbf{k}}^{AB,1}) & J_{\mathbf{k}}^{AB} \\ J_{\mathbf{k}}^{AB} & J_{\mathbf{k}}^{BB} - \epsilon(J_{\mathbf{k}}^{BB} - J_{\mathbf{k}}^{AB,2}) \end{pmatrix}. \quad (21)$$

Equation (17) can be expanded into two subseries,

$$\mathbf{G}_{\mathbf{k}\mathbf{k}'} = \mathbf{G}_{\mathbf{k}\mathbf{k}'}^{(1)} + \mathbf{G}_{\mathbf{k}\mathbf{k}'}^{(2)}, \quad (22)$$

where the subseries are, respectively,

$$\mathbf{G}_{\mathbf{k}\mathbf{k}'}^{(1)} = \mathbf{G}_{\mathbf{k}}^{vc} \rho_{\mathbf{k}-\mathbf{k}'} + \frac{1}{N} \sum_{\mathbf{q}} \mathbf{G}_{\mathbf{k}}^{vc} \mathbf{V}_{\mathbf{k}\mathbf{q}} \mathbf{G}_{\mathbf{q}}^{vc} \rho_{\mathbf{k}-\mathbf{q}} \rho_{\mathbf{q}-\mathbf{k}'} + \dots \quad (23)$$

and

$$\mathbf{G}_{\mathbf{k}\mathbf{k}'}^{(2)} = \left(\mathbf{G}_{\mathbf{k}}^{vc} \delta_{\mathbf{k}-\mathbf{k}'} + \mathbf{G}_{\mathbf{k}}^{vc} \mathbf{V}_{\mathbf{k}\mathbf{k}'} \mathbf{G}_{\mathbf{k}'}^{vc} \rho_{\mathbf{k}-\mathbf{k}'} \right. \\ \left. + \frac{1}{N} \sum_{\mathbf{q}} \mathbf{G}_{\mathbf{k}}^{vc} \mathbf{V}_{\mathbf{k}\mathbf{q}} \mathbf{G}_{\mathbf{q}}^{vc} \mathbf{V}_{\mathbf{q}\mathbf{k}'} \mathbf{G}_{\mathbf{k}'}^{vc} \rho_{\mathbf{k}-\mathbf{q}} \rho_{\mathbf{q}-\mathbf{k}'} + \dots \right) \\ \times \begin{pmatrix} c & 0 \\ 0 & c-1 \end{pmatrix}. \quad (24)$$

The averaged Green's function is obtained by averaging over products of ρ by expanding into cumulants $P_i(c)$. For instance,

$$\langle \rho_{\mathbf{k}_1} \rho_{\mathbf{k}_2} \rangle = \frac{P_2(c)}{N} \delta(\mathbf{k}_1 + \mathbf{k}_2), \quad (25)$$

$$\langle \rho_{\mathbf{k}_1} \rho_{\mathbf{k}_2} \rho_{\mathbf{k}_3} \rangle = \frac{P_3(c)}{N^2} \delta(\mathbf{k}_1 + \mathbf{k}_2 + \mathbf{k}_3), \quad (26)$$

and

$$\langle \rho_{\mathbf{k}_1} \rho_{\mathbf{k}_2} \rho_{\mathbf{k}_3} \rho_{\mathbf{k}_4} \rangle = \frac{P_4(c)}{N^3} \delta(\mathbf{k}_1 + \mathbf{k}_2 + \mathbf{k}_3 + \mathbf{k}_4) \\ + \left(\frac{P_2(c)}{N} \right)^2 [\delta(\mathbf{k}_1 + \mathbf{k}_2) \delta(\mathbf{k}_3 + \mathbf{k}_4) + \delta(\mathbf{k}_1 \\ + \mathbf{k}_3) \delta(\mathbf{k}_2 + \mathbf{k}_4) + \delta(\mathbf{k}_1 + \mathbf{k}_4) \delta(\mathbf{k}_2 + \mathbf{k}_3)]. \quad (27)$$

The cumulants are systematically obtained by the generating function

$$g(x,c) = \ln(1 - c + ce^x) = \sum_{i=1}^{\infty} P_i(c) \frac{x^i}{i!}. \quad (28)$$

From this equation one gets $P_1(c) = c$, $P_2(c) = c(1 - c)$, $P_3(c) = c(1 - c)(1 - 2c) \dots$.

In order to get a closed form for the series we have to make the usual CPA approximation which consists in keeping only the diagrams with no crossings of external lines. As it is was shown by Yonezawa⁷ and by Leath,⁸ the self-consistency requires a modification of the semi-invariants to be attributed to each vertex. In other words it means that the cumulants $P_i(c)$ have to be replaced by a new set of coefficients $Q_i(c)$ which satisfies the relation

$$Q_1(c) + Q_2(c)x + Q_3(c)x^2 \dots = \sigma_c(x) = \frac{c}{1 - x[1 - \sigma_c(x)]}, \quad (29)$$

where the modified cumulants are

$$Q_i(c) = \sum_{m=1}^i \binom{i+m-2}{m-1} (-1)^{m-1} \frac{(i+m-2)!}{m!(i-m)!(m-1)!} c^m. \quad (30)$$

In the single-site approximation, after averaging, one gets for the averaged 2×2 Green's-function matrix

$$\bar{\mathbf{G}}_{\mathbf{k}\mathbf{k}'} = \bar{\mathbf{G}}_{\mathbf{k}} \delta_{\mathbf{k}-\mathbf{k}'} = \tilde{\mathbf{G}}_{\mathbf{k}} \left[\begin{pmatrix} c & 0 \\ 0 & c-1 \end{pmatrix} + \mathbf{\Delta}_{\mathbf{k}} \right], \quad (31)$$

where

$$\tilde{\mathbf{G}}_{\mathbf{k}} = [(\mathbf{G}_{\mathbf{k}}^{vc})^{-1} - \mathbf{\Sigma}_{\mathbf{k}}]^{-1}. \quad (32)$$

$\mathbf{\Sigma}_{\mathbf{k}}$ denotes the self-energy; it is given by

$$\mathbf{\Sigma}_{\mathbf{k}} = Q_2 \frac{1}{N} \sum_{\mathbf{q}} \mathbf{V}_{\mathbf{k}\mathbf{q}} \tilde{\mathbf{G}}_{\mathbf{q}} \mathbf{V}_{\mathbf{q}\mathbf{k}} + Q_3 \frac{1}{N^2} \sum_{\mathbf{q},\mathbf{t}} \mathbf{V}_{\mathbf{k}\mathbf{q}} \tilde{\mathbf{G}}_{\mathbf{q}} \mathbf{V}_{\mathbf{q}\mathbf{t}} \tilde{\mathbf{G}}_{\mathbf{t}} \mathbf{V}_{\mathbf{t}\mathbf{k}} + \dots \quad (33)$$

and

$$\mathbf{\Delta}_{\mathbf{k}} = Q_2 \frac{1}{N} \sum_{\mathbf{q}} \mathbf{V}_{\mathbf{k}\mathbf{q}} \tilde{\mathbf{G}}_{\mathbf{q}} + Q_3 \frac{1}{N^2} \sum_{\mathbf{q},\mathbf{t}} \mathbf{V}_{\mathbf{k}\mathbf{q}} \tilde{\mathbf{G}}_{\mathbf{q}} \mathbf{V}_{\mathbf{q}\mathbf{t}} \tilde{\mathbf{G}}_{\mathbf{t}} + \dots \quad (34)$$

The term $\mathbf{\Delta}_{\mathbf{k}}$ which is very similar to the self-energy is called end correction.⁹ Note that, inside the CPA loop, Eqs. (32) and (33) are the only two equations which have to be solved self-consistently. To summarize, in Fig. 1 we show a diagrammatic representation of the previous set of equations.

A. Evaluation of $\mathbf{\Delta}_{\mathbf{k}}$

It is convenient for the calculations to start by defining

$$\gamma_i(\mathbf{q}) = \frac{1}{z_i} \sum_{\mathbf{r}_i^j} \exp(i\mathbf{q}\mathbf{r}_i^j). \quad (35)$$

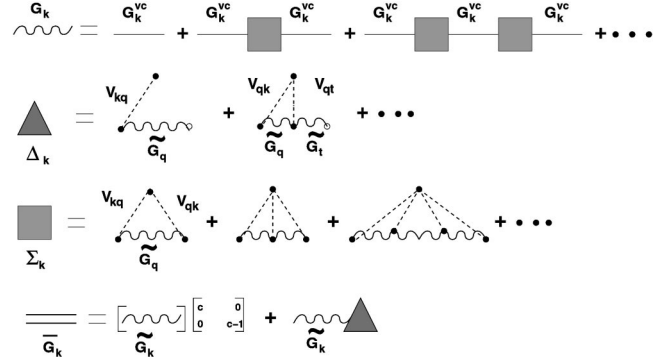


FIG. 1. Diagrammatic representation of the averaged Green's function calculated within the CPA loop. $\bar{\mathbf{G}}$ is the total averaged Green's function, $\mathbf{\Sigma}_{\mathbf{k}}$ is the self-energy, and $\mathbf{\Delta}_{\mathbf{k}}$ the end-correction.

The sum \mathbf{r}_i^j runs over the i th type of neighbors of the i th shell E_i from a given site 0 and z_i is the total number of neighbors in the shell. Note that from now on Σ_i will correspond to a summation over the different shells. With this definition it follows immediately that,

$$J^{AA}(\mathbf{q}) = \sum_i J_{oi}^{AA} z_i \gamma_i(\mathbf{q}). \quad (36)$$

We get a similar expression for $J^{BB}(\mathbf{q})$ and $J^{AB}(\mathbf{q}) \dots$.

It is convenient to decompose the matrix $\mathbf{V}_{\mathbf{k}\mathbf{q}}$ into two terms,

$$\mathbf{V}_{\mathbf{k}\mathbf{q}} = \mathbf{V}_{\mathbf{k}\mathbf{q}}^{(1)} + \mathbf{V}_{\mathbf{k}\mathbf{q}}^{(2)}, \quad (37)$$

where

$$\mathbf{V}_{\mathbf{k}\mathbf{q}}^{(1)} = \sum_i \mathbf{V}_{\mathbf{k}\mathbf{q}}^{(1),i} = \sum_i [\mathbf{A}_i - \epsilon \mathbf{D}_i \gamma_i(\mathbf{k})] \gamma_i(\mathbf{q}) \quad (38)$$

and

$$\mathbf{V}_{\mathbf{k}\mathbf{q}}^{(2)} = \sum_i \mathbf{V}_{\mathbf{k}\mathbf{q}}^{(2),i} = \epsilon \mathbf{D}_i [\gamma_i(\mathbf{k}) \gamma_i(\mathbf{q}) - \gamma_i(\mathbf{k}-\mathbf{q})]. \quad (39)$$

\mathbf{A}_i and \mathbf{D}_i are the following 2×2 matrices:

$$\mathbf{A}_i = \begin{pmatrix} J_{oi}^{AA} & J_{oi}^{AB} \\ J_{oi}^{AB} & J_{oi}^{BB} \end{pmatrix} z_i, \quad (40)$$

$$\mathbf{D}_i = \begin{pmatrix} J_{oi}^{AA} - J_{oi}^{AB,1} & 0 \\ 0 & J_{oi}^{BB} - J_{oi}^{AB,2} \end{pmatrix} z_i. \quad (41)$$

By using the following very useful property,¹⁶ if $f(r)$ is a function which is equivalent at each site r_i of the i th shell E_i , then

$$\frac{1}{N} \sum_{\mathbf{q}} \gamma_i(\mathbf{k}-\mathbf{q}) f(\mathbf{q}) = \gamma_i(\mathbf{k}) \frac{1}{N} \sum_{\mathbf{q}} \gamma_i(\mathbf{q}) f(\mathbf{q}). \quad (42)$$

By using Eq. (42), we find significant simplifications in the calculations. Indeed, all the terms of the sum involving at

least one factor $\mathbf{V}^{(2)}$ reduces to zero. Thus the end correction term does not explicitly depend on the environmental disorder term.

After calculation we finally get

$$\Delta_{\mathbf{k}} = \sum_{ij} \mathbf{V}_{\mathbf{k},0}^{(1),i} [Q_2 \mathbf{I} + Q_3 \mathbf{M} + Q_4 \mathbf{M}^2 + \dots]_{ij} \mathbf{F}^j. \quad (43)$$

Like $\mathbf{V}^{(1),i}$, \mathbf{F}^j is a 2×2 matrix, and \mathbf{M} a $N_s \times N_s$ matrix, where each matrix element \mathbf{M}_{ij} is a 2×2 matrix. N_s denotes the number of considered shells. $\mathbf{V}^{(1),i}$ is given in Eq. (38) and \mathbf{F}^j and \mathbf{M}_{ij} are defined by

$$\mathbf{F}^i = \frac{1}{N} \sum_{\mathbf{q}} \gamma_i(\mathbf{q}) \tilde{\mathbf{G}}_{\mathbf{q}} \quad (44)$$

and

$$\mathbf{M}_{ij} = \frac{1}{N} \sum_{\mathbf{q}} \gamma_i(\mathbf{q}) \tilde{\mathbf{G}}_{\mathbf{q}} \mathbf{V}_{\mathbf{q},0}^{(1),j}. \quad (45)$$

The sum in Eq. (43) is obtained after diagonalization of the $2N_s \times 2N_s$ matrix $\mathbf{M} = \mathbf{P}^{-1} \mathbf{M}_{diag} \mathbf{P}$,

$$Q_2 \mathbf{I} + Q_3 \mathbf{M} + Q_4 \mathbf{M}^2 + \dots = \mathbf{P}^{-1} \{ [\sigma_c(\mathbf{M}_{diag}) - Q_1 \mathbf{I}] \mathbf{M}_{diag}^{-1} \} \mathbf{P}. \quad (46)$$

The function σ_c was previously defined in Eq. (29), and $[\sigma_c(\mathbf{M}_{diag})]_{ij} = \sigma_c(\lambda_i) \delta_{ij}$ where λ_i are the eigenvalues of \mathbf{M} . Hence we get for the end correction

$$\Delta_{\mathbf{k}} = \sum_{ij} \mathbf{V}_{\mathbf{k},0}^{(1),i} (\mathbf{P}^{-1} \{ [\sigma_c(\mathbf{M}_{diag}) - Q_1 \mathbf{I}] \mathbf{M}_{diag}^{-1} \} \mathbf{P})_{ij} \mathbf{F}^j. \quad (47)$$

Let us now proceed further and evaluate the self-energy $\Sigma_{\mathbf{k}}$.

B. Evaluation of $\Sigma_{\mathbf{k}}$

Using the remarks made in the previous section, we find that the self-energy can be written

$$\Sigma_{\mathbf{k}} = \Sigma_{\mathbf{k}}^{(1)} + \Sigma_{\mathbf{k}}^{(2)}, \quad (48)$$

where $\Sigma_{\mathbf{k}}^{(1)}$ (respectively $\Sigma_{\mathbf{k}}^{(2)}$) is obtained by replacing $\mathbf{V}_{\mathbf{k},\mathbf{q}}$ by $\mathbf{V}_{\mathbf{k},\mathbf{q}}^{(1)}$ (respectively $\mathbf{V}_{\mathbf{k},\mathbf{q}}^{(2)}$). Indeed we find that each term of the sum containing both $\mathbf{V}^{(1)}$ and $\mathbf{V}^{(2)}$ reduces to zero. After simplifications we obtain for $\Sigma_{\mathbf{k}}^{(1)}$,

$$\Sigma_{\mathbf{k}}^{(1)}(\mathbf{k}) = \sum_{i,j} \mathbf{V}_{\mathbf{k},0}^i [Q_1 \mathbf{I} + Q_2 \mathbf{M} + Q_3 \mathbf{M}^2 + \dots]_{ij} \Gamma^j(\mathbf{k}), \quad (49)$$

where $\Gamma^j(\mathbf{k}) = \gamma_j(\mathbf{k}) \begin{pmatrix} 1 & 0 \\ 0 & 1 \end{pmatrix}$.

As previously done for the end correction, using the function $\sigma_c(z)$ defined in Eq. (29) we obtain immediately

$$Q_1 \mathbf{I} + Q_2 \mathbf{M} + Q_3 \mathbf{M}^2 + \dots = \mathbf{P}^{-1} [\sigma(\mathbf{M}_{diag})] \mathbf{P}. \quad (50)$$

Note that we have included in the sum the first-order term depending on c (Q_1) which comes from the virtual crystal Green's function \mathbf{G}_q^{vc} .

In general, the evaluation of the second term $\Sigma^{(2)}(\mathbf{k})$ is much more complicated. One can get an analytical form only for simple cases. For example, if the exchange integrals are restricted to only nearest neighbors, the complete summation of the sum can be performed by using the space-group symmetry of the lattice.^{9,17} In the case of nearest-neighbor Heisenberg system one gets

$$\Sigma_{\mathbf{k}}^{(2)}(E) = C_p [1 - \gamma(2\mathbf{k})] + C_d [1 + \gamma(2\mathbf{k}) - 2\gamma(\mathbf{k})^2], \quad (51)$$

where

$$C_{p,d} = -\frac{\epsilon}{2} (Q_1 \mathbf{I} + Q_2 \mathbf{M}_{p,d} + Q_3 \mathbf{M}_{p,d}^2 + \dots) \mathbf{D}_1. \quad (52)$$

$C_{p,d}$ are evaluated in the same way that it was done for $\Sigma_{\mathbf{k}}^{(1)}(E)$ and $\Delta_{\mathbf{k}}(E)$. The matrices \mathbf{D}_1 , \mathbf{M}_p , and \mathbf{M}_d are, respectively,

$$\mathbf{D}_1 = \begin{pmatrix} J^{AA} - J^{AB,1} & 0 \\ 0 & J^{BB} - J^{AB,2} \end{pmatrix} z, \quad (53)$$

$$\mathbf{M}_p = -\frac{\epsilon}{6} \mathbf{D}_1 \tilde{\mathbf{G}}_p, \quad (54)$$

$$\mathbf{M}_d = -\frac{\epsilon}{4} \mathbf{D}_1 \tilde{\mathbf{G}}_d, \quad (55)$$

where $\tilde{\mathbf{G}}_p = (1/N) \sum_{\mathbf{q}} [1 - \gamma(2\mathbf{q})] \tilde{\mathbf{G}}(\mathbf{q})$ and $\tilde{\mathbf{G}}_d = (1/N) \sum_{\mathbf{q}} [1 + \gamma(2\mathbf{q}) - 2\gamma(\mathbf{q})^2] \tilde{\mathbf{G}}(\mathbf{q})$.

Note that the virtual crystal approximation for $\Sigma_{\mathbf{k}}^{(2)}(E)$ consists of taking in Eq. (52) the first term only. Then it follows immediately that,

$$C_p^{VCA} = C_d^{VCA} = -\frac{\epsilon c}{2} \mathbf{D}_1 \quad (56)$$

which substituted in Eq. (51) leads to

$$\Sigma_{\mathbf{k}}^{(2),VCA}(E) = -\epsilon c \mathbf{D}_1 [1 - \gamma(\mathbf{k})^2]. \quad (57)$$

Note that $\Sigma_{\mathbf{k}}^{(2),VCA}$ is energy independent. It is also important to stress that at the lowest order the self-consistency for $\Sigma^{(2)}$ is not required.

Most of the ferromagnetic materials are of itinerant type, which means that the exchange integrals between different localized magnetic ions are long range and driven by the polarization of the conduction electrons gas as it is for the Ruderman-Kittel-Kasuya-Yosida (RKKY) mechanism.¹⁸ Analytically, the generalization of the previous calculations to the more interesting case where J_{ij} are long ranged is not an easy task. However, by truncating the sum, the summation can be performed numerically. It is important to note that $\Sigma^{(2)}(\mathbf{k})$ is (i) proportional to ϵ which means that it originates only from the environmental disorder term, and (ii) each term of the sum vanishes in the long-wavelength limit $\Sigma^{(2)}(\mathbf{k}=\mathbf{0})=0$. This implies that even after truncation of the sum at any order, the Goldstone theorem remains fulfilled. Thus the long-wavelength magnons are always treated prop-

erly. Furthermore, since $\Sigma^{(2)}(\mathbf{k})$ corresponds to higher-order scattering terms (p, d, f, \dots) it is natural to expect that these terms should not affect the Curie temperature in a dramatic way. In other words, we expect that a truncation of $\Sigma^{(2)}(\mathbf{k})$ sum to the first few terms should already provide a good approximation of Curie temperature compared to the one obtained with the complete series. However, it is crucial to consider at least the lowest-order term (the virtual crystal contribution), otherwise even in the clean limit one would not recover the correct result and the Goldstone's theorem would be violated. If we consider the lower approximation $\Sigma^{(2)} \approx \Sigma_{VCA}^{(2)}$, we get the expected results in the limit $c=0$ and $c=1$. It is not *a priori* clear whether such an approximation of $\Sigma^{(2)}(\mathbf{k})$ to the lowest order provides satisfying results for the Curie temperature at moderate impurity concentration. Such an approximation will be tested later on.

To conclude this section, the complete averaged 2×2 Green's function is obtained after solving self-consistently the set of Eqs. (32) and (33) within the CPA loop and then using Eqs. (31) and (34) to get $\Delta_{\mathbf{k}}$ and $\bar{\mathbf{G}}_{\mathbf{k}}$. However, as was already mentioned in the introduction, the problem is not solved until we are able to calculate the locators g_{λ}^0 and the exchanged integrals Ψ_{il} which depend on the averaged magnetization m_{λ} . The determination of m_{λ} has to be done self-consistently in an additional external loop (RPA).

IV. MAGNETIZATION AND CURIE TEMPERATURE

We assume that the averaged 2×2 Green's function matrix $\bar{\mathbf{G}}(\mathbf{k}, E)$ is calculated according to the previous section within the CPA loop. We show how from $\bar{G}_{\lambda}(\mathbf{k}, E)$, $\lambda=A$ or B we can get the missing self-consistent equations (RPA loop) to get the temperature-dependent locator g_{λ}^0 and the exchange integrals Ψ_{il} . This will allow us to calculate the element-resolved magnetizations $m_{\lambda} = \langle S_{\lambda}^z \rangle$ as a function of temperature and the Curie temperature. It was shown by Callen, in the case of a clean system (pure A or B), that the magnetization can be expressed in the following way:¹⁶

$$m_{\lambda} = \frac{(S_{\lambda} - \Phi_{\lambda})(1 + \Phi_{\lambda})^{2S_{\lambda}+1} + (S_{\lambda} + 1 + \Phi_{\lambda})\Phi_{\lambda}^{2S_{\lambda}+1}}{(1 + \Phi_{\lambda})^{2S_{\lambda}+1} - \Phi_{\lambda}^{2S_{\lambda}+1}}, \quad (58)$$

where $\Phi_{\lambda} = (1/N) \sum_{\mathbf{q}} \Phi_{\lambda}(\mathbf{q})$ and $\Phi_{\lambda}(\mathbf{q})$ is defined as

$$\Phi_{\lambda}(\mathbf{q}) = \int_{-\infty}^{+\infty} dE \frac{A_{\lambda}(\mathbf{q}, E)}{e^{2mE/kT} - 1}, \quad (59)$$

where

$$A_{\lambda}(\mathbf{q}, E) = \frac{-1}{\pi} \text{Im} \bar{G}_{\lambda}^{+-}(\mathbf{q}, E) \quad (60)$$

is the spectral function.

Note also that the Callen's approach to get the magnetization allows us to derive a lot of local spin-spin correlations; they are only expressed as a function of Φ_{λ} . For instance,

$$\langle (S_{\lambda}^z)^2 \rangle = S(S+1) - m_{\lambda}(1 + 2\Phi_{\lambda}) \quad (61)$$

which is needed to determine the anisotropy parameters γ_{λ} given in Eq. (8).

In the case of clean systems, the normalized spectral function $A_{\lambda}(\mathbf{q}, E)$ is given by

$$A_{\lambda}(\mathbf{q}, E) = \delta[E - E(\mathbf{q})], \quad (62)$$

$E(\mathbf{q}) = \omega(\mathbf{q})/2m$ and $\omega(\mathbf{q})$ denotes the magnon dispersion.

In the case of a binary (or multicomponent) alloy this formula can be generalized in the following way:

$$A_{\lambda}(\mathbf{q}, E) = \frac{-1}{\pi} \frac{\text{Im} \bar{G}_{\lambda}^{+-}(\mathbf{q}, E)}{c_{\lambda} x_{\lambda}}, \quad (63)$$

where c_{λ} is the concentration of the λ ion and we have for convenience introduced a T -dependent reduced variable $x_{\lambda} = m_{\lambda}/m$.

Note that in the presence of impurities the spectral function is no longer a δ function, but because of the finite imaginary part of the self-energy it will consist of peaks of finite width with a more or less Lorentzian shape. In the case of binary alloys we expect for a given \mathbf{q} two peaks, more generally n peaks for an n -component alloy.

For a given temperature the complete self-consistency is obtained by (i) providing good starting values for m_{λ} , then (ii) performing the CPA loop which provide $\bar{\mathbf{G}}(\mathbf{k}, E)$, and finally (ii) going into the RPA loop by using Eqs. (58), (61), and (63) one gets the new values of m_{λ} and $\langle (S_{\lambda}^z)^2 \rangle$ which are re-injected in the locators g_{λ}^0 , the exchange integrals Ψ_{il} , and γ_{λ} .

Let us now show how to get the Curie temperature of a disordered Heisenberg binary alloy. We start by expanding Eq. (59) in the limit $T \rightarrow T_C$ (i.e., $m_{\lambda} \rightarrow 0$). We immediately get

$$\Phi_{\lambda} \approx \frac{kT_C}{2m} F_{\lambda}, \quad (64)$$

where

$$F_{\lambda} = \frac{1}{N} \sum_{\mathbf{q}} \int_{-\infty}^{+\infty} dE \frac{A_{\lambda}(\mathbf{q}, E)}{E}. \quad (65)$$

After expanding Eq. (58) as a function of $1/\Phi_{\lambda}$ one obtains

$$m_{\lambda} = \frac{S_{\lambda}(S_{\lambda}+1)}{3} \frac{2m}{kT_C} \frac{1}{F_{\lambda}}. \quad (66)$$

Since the averaged magnetization m is defined by $m = \sum_{\lambda} c_{\lambda} m_{\lambda}$, combining the two previous equations one finds for the Curie temperature

$$k_B T_C = \frac{2}{3} \sum_{\lambda} c_{\lambda} \frac{S_{\lambda}(S_{\lambda}+1)}{F_{\lambda}}. \quad (67)$$

Equation (67) is the RPA generalization of the Curie temperature to a multicomponent disordered alloy. The previous

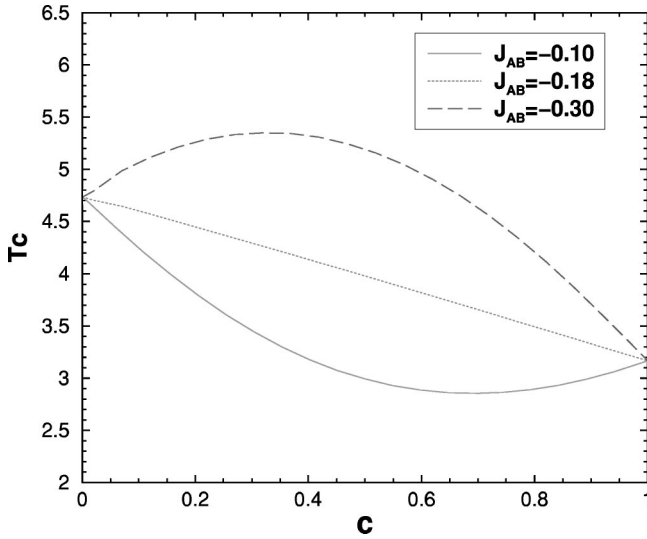


FIG. 2. Curie temperature T_C for disordered nearest-neighbor Heisenberg ferromagnet as a function of the impurity concentration $c(A)$. The parameters are $S_A=2$, $S_B=3$, $J_{AA}=-0.2$, and $J_{BB}=-0.15$. We have chosen three different values for J_{AB} .

equation provides a direct measure of the weight $w_\lambda = (1/k_B T_C) \{c_\lambda [S_\lambda(S_\lambda + 1)/F_\lambda]\}$ of each λ element to the Curie temperature.

V. NUMERICAL RESULTS

In this section we provide an illustration of the RPA-CPA theory and a test for the approximation suggested above for the higher-order scattering contribution of the self-energy. For simplicity, we consider the case of a 3D disordered binary alloy on a simple cubic lattice. Additionally we restrict the exchange integrals to nearest neighbor only which allows us to test the validity of the approximation scheme suggested in Sec. III before estimating Σ^2 . For further simplifications of the calculations we consider the case of a zero external field and neglect the anisotropy term which is reasonable for a 3D system.

In Fig. 2, we have plotted the Curie temperature as a function of c obtained with the full CPA treatment; the $\Sigma^{(2)}$ part of the self-energy is calculated exactly (full summation of the sum). Note that pure A (respectively B) corresponds to $c=1$ (respectively $c=0$). Depending on the chosen set of parameters T_C shows (i) a minimum [$J_{AB}S_A S_B \leq \min(J_{AA}S_A^2, J_{BB}S_B^2)$], (ii) a maximum [$J_{AB}S_A S_B \geq \max(J_{AA}S_A^2, J_{BB}S_B^2)$], or (iii) is monotonic [$\min(J_{AA}S_A^2, J_{BB}S_B^2) \leq J_{AB}S_A S_B \leq \max(J_{AA}S_A^2, J_{BB}S_B^2)$]. These three different cases are shown in the figure.

As already mentioned in Sec. III, it is difficult to perform the full summation of $\Sigma^{(2)}$ for the case of long-range exchange integrals which is the case of many realistic and interesting systems, for example permalloy. As it was discussed previously, the simplest approximation consists of keeping only the lowest-order term of the sum (virtual crystal approximation). In the case of the nearest-neighbor Heisenberg system, $\Sigma^{(2)}$ and $\Sigma^{(2),VCA}$ are respectively given in Eqs. (51) and (57). In Fig. 3 we have plotted the Curie

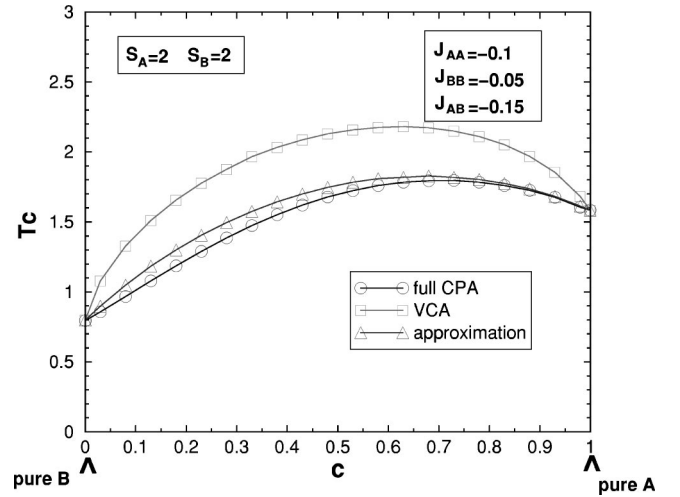


FIG. 3. Comparison between the Curie temperature calculated as function of the impurity concentration for a nearest-neighbor Heisenberg ferromagnet. (a) The full CPA calculation, (b) approximation for $\Sigma^{(2)} = \Sigma_{VCA}^{(2)}$, and (c) the virtual crystal calculation. The chosen set of parameters is written in the figure.

temperature calculated with (i) a full CPA treatment, (ii) the one performed with the approximation discussed previously, $\Sigma^{(2)} = \Sigma_{VCA}^{(2)}$, and (iii) the one obtained with virtual crystal approximation. In case (iii), the averaged Green's function is

$$\bar{\mathbf{G}}_{\mathbf{k}} = \mathbf{G}_{\mathbf{k}}^{vc} \begin{pmatrix} c & 0 \\ 0 & c-1 \end{pmatrix} \quad (68)$$

since in VCA $\Delta_{\mathbf{k}} = 0$.

The comparison between the full CPA and the virtual crystal approximation (VCA) shows that the Curie temperature differs significantly. Even very close to the clean limit the VCA appears to be inappropriate, for instance for $c=0.1$ we observe that T_C^{VCA} is about 35% larger than the full CPA calculated one. Note that the disagreement is even more pronounced in the vicinity of $c=0$ than $c=1$. This can be understood in the following way: since $J_{AB} = 3J_{BB} = 1.5J_{AA}$ and $S_A = S_B$ a substitution of a B site by an A site (close to $c=0$) introduces a change of energy (with respect to the pure case) two times larger than a substitution of a B site by an A site near $c=1$. As discussed previously, it is interesting to compare the Curie temperature where the VCA is only done on $\Sigma^{(2)}$ ($T_c^{2,VCA}$). We observe a good agreement between the full CPA calculated T_C and $T_c^{2,VCA}$, in the whole range of concentration; the agreement is even excellent for $c \geq 0.6$. A comparison between T_C^{VCA} and $T_c^{2,VCA}$ in the vicinity of $c=0$ and $c=1$ shows that the reason why the VCA approximation breaks down is essentially because of the crude approximation of the s part of the scattering. Thus this figure validates a simple treatment of $\Sigma^{(2)}$. It is also expected that including only a few additional terms of the sum will lead to an excellent agreement in the whole range of concentration.

In Fig. 4 we show the temperature dependence of the element-resolved magnetizations. In order to demonstrate the versatility of our approach, we have chosen a set of param-

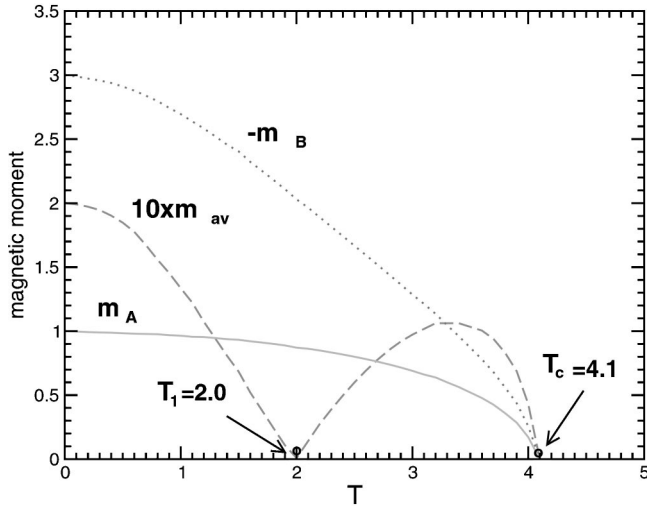


FIG. 4. Magnetizations m_A , $-m_B$, and averaged one $c_{av} = |c_A m_A + c_B m_B|$ as a function of temperature. The spins are $S_A = 1$ and $S_B = 3$, the exchange couplings are $J_{AA} = -1.2$, $J_{BB} = -0.10$, and an antiferromagnetic coupling between A and B is taken $J_{AB} = 0.15$. The concentration of A atoms is $c_A = 0.70$.

eters which mimics a ferrimagnetic behavior with compensation point. Additionally, the parameters are such that $T_C^A \gg T_C^B$. While the temperature dependence of m_A follows a standard behavior, $m_B(T)$ starts to strongly decrease even at low temperature. For example, at $T \approx 2.5$, m_A is reduced by less than 20% while $m_B = 0.5 m_B(0)$. As a result of our choice of parameters we see that the averaged magnetization $m_{av} = |c_A m_A + c_B m_B|$ is nonmonotonic and vanishes for an intermediate temperature value (compensation point). It is found that the function $(m_B/m_A)(T)$ decreases monotonically

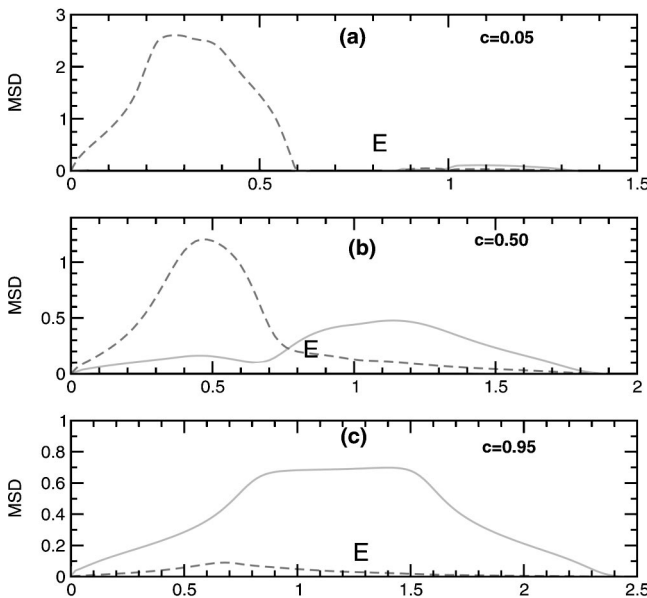


FIG. 5. Magnetic spectral density $\rho_\lambda(E) = \text{Im}G^\lambda(E)/x_\lambda c_\lambda$ as a function of E . The continuous line corresponds to $\lambda = A$ and the dashed line to $\lambda = B$ for three different concentration of A : $c = 0.05$, 0.5 , and 0.95 . The parameters are $S_A = 2$, $S_B = 3$, $J_{AA} = -0.2$, $J_{BB} = -0.05$, $J_{AB} = -0.15$, and $T \approx T_C$.

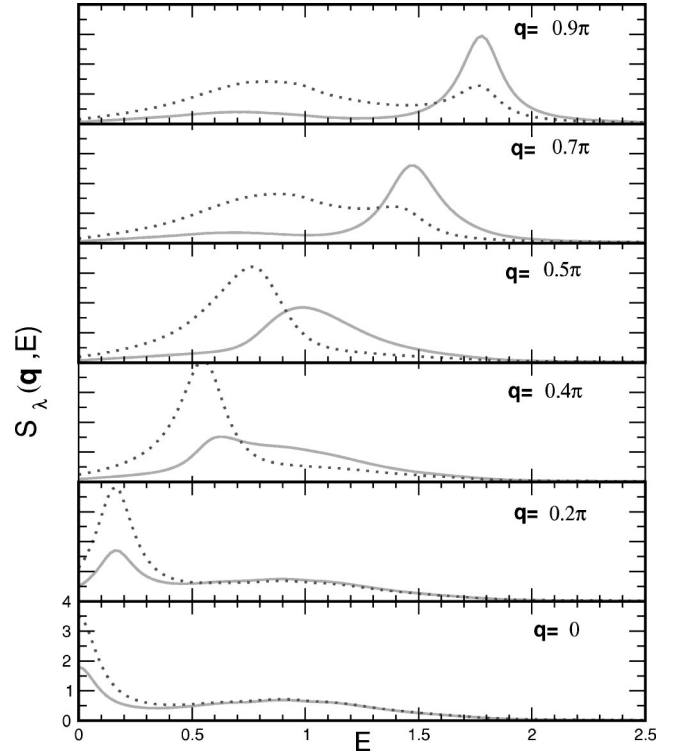


FIG. 6. Spectral function $S_\lambda(\mathbf{q}, E) = -(1/\pi) \text{Im}G^\lambda(\mathbf{q}, E)$ as a function of E for different momentum \mathbf{q} where $\mathbf{q} = q(1,1,1)$. The continuous line corresponds to $\lambda = A$ and the dashed line to $\lambda = B$. The spins are $S_A = 2$ and $S_B = 3$, the exchange couplings are $J_{AA} = -0.2$, $J_{BB} = -0.10$, $J_{AB} = -0.15$, and $c_A = 0.50$. We have taken $T \approx T_C$. For clarity of the picture a small imaginary part $\eta = 0.1$ have been added.

ally with temperature. As a result, and since at $T = 0$, $m_B/m_A = S_B/S_A$, thus if $S_B/S_A \leq c_A/c_B$ then m_{av} will not have a compensation point. However, the condition that $S_B/S_A \geq c_A/c_B$ is not sufficient to get one, it is also required that $m_B/m_A(T_C) \leq c_A/c_B$.

In Fig. 5 we now show the magnon spectral density (MSD) $\rho_\lambda(E) = \text{Im}G^\lambda(E)/x_\lambda c_\lambda$ as a function of E . We consider three different cases: almost clean A and B [(a) and (c)], and the intermediate situation $c_A = c_B = 0.5$. In both Figs. 5(a) and (c) we observe that the MSD is very similar to the clean case. This is clearer in case (c) than (a); it is easy to understand that when doping A with B the difference in energy with the undoped case is only of order 10% [$J_{AA}(S_A)^2 = 0.8$ and $J_{AB}S_A S_B = 0.9$] while when doping B with A the change is more drastic (about 100%). To get a similar MSD to Fig. 5(c) for a weakly doped B sample, one should take $c \approx 0.005$.

In Fig. 6 we show the spectral function $S_\lambda(\mathbf{q}, E)$ as a function of energy for different values of the momentum \mathbf{q} . This quantity is more interesting that the integrated MSD since it provides direct information about the elementary excitation dispersions and their spectral weight. Additionally it is directly related to inelastic neutron-scattering measurements. Let us now briefly discuss Fig. 6. At precisely $\mathbf{q} = \mathbf{0}$ momentum, in both $S_{\lambda=A,B}$, we observe two peak structures: (i) a well defined peak¹⁹ at $E = 0$, as expected since our

theory fulfills the Goldstone theorem, and (ii) a very broad one at intermediate energy $E \approx 1$. For intermediate values of the momentum, it is difficult to separate the peak and one get a single broad peak. We see clearly that the peaks are crossing each other at $\mathbf{q} \approx (\pi/2)(1,1,1)$. Note that due to (i) the different spectral weight of the peaks and to the closeness of their location, the single peak-structure which is observed at $q = \pi/2$ is located at different energies for A and B . From this figure we see also that the dispersion of the second peak is almost flat $E_2(q) \approx 1$, while the Goldstone mode $E_1(\mathbf{q})$ (Ref. 20) goes from $E=0$ to $E_{max} \approx 2$ when moving in the $(1,1,1)$ direction.

VI. CONCLUSION

In conclusion, we have presented in this paper a theory based on Green's-function formalism to study magnetism in

disordered Heisenberg systems with long-range exchange integrals. The disordered Green's function are decoupled within the Tyablicov procedure and the disorder (*diagonal*, *off-diagonal*, and *environmental*) is treated with a 2×2 modified cumulant CPA approach. The crucial point is that we are able to treat simultaneously and self-consistently the RPA and CPA loops. Our theory allows us in particular to calculate Curie temperature, spectral functions, and temperature dependence of the magnetization for each element as a function of concentration of impurity. Additionally, we have proposed a simplified treatment of the $p, d, f \dots$ contribution of the self-energy which is difficult to handle in the case of long-range exchange integrals. The approximation was tested successfully on 3D disordered nearest-neighbor Heisenberg systems. Combined with first-principle calculations which can provide the exchange integrals, this method appears to be very promising to study magnetism in disordered systems.

-
- ¹R.J. Elliott, B.R. Leath, and J.A. Krumhansl, Rev. Mod. Phys. **46**, 465 (1974).
²F. Yonezawa and K. Morigaki, Suppl. Prog. Theor. Phys. **53**, 1 (1973).
³P. Soven, Phys. Rev. **156**, 809 (1967).
⁴D.W. Taylor, Phys. Rev. **156**, 1017 (1967).
⁵J.A. Blackman, D.M. Esterling, and N.F. Berk, Phys. Rev. B **4**, 2412 (1971).
⁶A. Gonis and J.W. Garland, Phys. Rev. B **16**, 1495 (1977).
⁷F. Yonezawa, Prog. Theor. Phys. **40**, 34 (1968).
⁸P.L. Leath, Phys. Rev. **171**, 725 (1968).
⁹E.J.S. Lage and R.B. Stinchcombe, J. Phys. C **10**, 295 (1977).
¹⁰D.J. Whitelaw, J. Phys. C **14**, 2871 (1981).
¹¹M. Pajda, J. Kudrnovský, I. Turek, V. Drchal, and P. Bruno, Phys. Rev. Lett. **85**, 5424 (2000); Phys. Rev. B **64**, 174402 (2001).
¹² $J_{ij}^{\lambda\lambda'}$ denotes the exchange integral between an atom of type λ at site i and a λ' atom at site j , both immersed in the effective medium. This implies that $J_{ij}^{\lambda\lambda'} = J_{|i-j|}^{\lambda\lambda'}$.
¹³S.V. Tyablicov, *Methods in Quantum Theory of Magnetism* (Plenum Press, New York, 1967).
¹⁴P. Fröbrich, P.J. Jensen, and P.J. Kuntz, Eur. Phys. J. B **13**, 477 (2000).
¹⁵F.B. Anderson and H.B. Callen, Phys. Rev. A **136**, A1068 (1964).
¹⁶H.B. Callen, Phys. Rev. **130**, 890 (1963); see also H.B. Callen and S. Shtrikman, Solid State Commun. **5**, 5 (1965).
¹⁷Y. Izyumov, Proc. Phys. Soc. Jpn. **87**, 505 (1966).
¹⁸A.A. Rudermann and C. Kittel, Phys. Rev. **96**, 99 (1954); T. Kasuya, Prog. Theor. Phys. **16**, 45 (1956); K. Yosida, Phys. Rev. **106**, 893 (1957).
¹⁹For convenience a small broadening has been introduced to make the figure easier for the reader. At exactly $q=0$ we find that the peak at $E=0$ is a δ peak consistent with the fact that $\text{Im}G_\lambda(E=0)=0$.
²⁰As expected, analyzing closely $S_\lambda(\mathbf{q}, E)$ in the vicinity of $q=0$, we find that $E_1(\mathbf{q}) = Dq^2$.